J Membrane Biol (2010) 236:117–125
DOI 10.1007/s00232-010-9283-0

Hollow Microneedle Arrays for Intradermal Drug Delivery and DNA Electroporation

Liévin Daugimont · Nolwenn Baron · Gaëlle Vandermeulen · Natasa Pavselj · Damijan Miklavcic · Marie-Caroline Jullien · Gonzalo Cabodevila · Lluis M. Mir · Véronique Préat

Received: 5 January 2010 / Accepted: 22 June 2010 / Published online: 22 July 2010

Abstract The association of microneedles with electric pulses causing electroporation could result in an efficient and less painful delivery of drugs and DNA into the skin. Hollow conductive microneedles were used for (1) needle-free intradermal injection and (2) electric pulse application in order to achieve electric field in the superficial layers of the skin sufficient for electroporation. Microneedle array was used in combination with a vibratory inserter to disrupt the stratum corneum, thus piercing the skin. Effective injection of proteins into the skin was achieved, resulting in an immune response directed to the model antigen ovalbumin. However, when used both as microneedles to inject and as electrodes to apply the electric pulses, the setup showed several limitations for DNA electrotransfer. This could be due to the distribution of the electric field in the skin as shown by numerical calculations and/or the low dose of DNA injected. Further investigation of these parameters is needed in order to optimize minimally invasive DNA electrotransfer in the skin.

Keywords Microneedle · Skin · Electroporation · Drug delivery · DNA · Electric field distribution

The first two authors contributed equally to this work.

L. Daugimont · G. Vandermeulen · V. Préat (✉)
Louvain Drug Research Institute, Unité de pharmacie galénique, Université Catholique de Louvain, Avenue E. Mounier 73/20, 1200 Brussels, Belgium
e-mail: veronique.preat@uclouvain.be

N. Baron · G. Cabodevila
Département MN2S, Institut FEMTO-ST, UMR CNRS 6174, ENSMM, Besançon, France

N. Pavselj · D. Miklavcic
Faculty of Electrical Engineering, University of Ljubljana, Ljubljana, Slovenia

M.-C. Jullien
CNRS UMR 8029, SATIE, ENS Cachan Bretagne, Bruz, France

L. M. Mir
CNRS UMR 8203, Institut Gustave-Roussy, Villejuif and Université Paris-Sud, Orsay, France

Introduction

The number of biotechnology-based drugs and vaccines is dramatically increasing. These macromolecules are usually delivered by injection. Hence, the development of noninvasive, user-friendly delivery methods remains a major challenge.

Transdermal delivery is an appealing alternative for the delivery of biotechnology-based drugs. However, it is limited by the low permeability of the skin. Different chemical, mechanical and physical methods have been developed to overcome this barrier (Vandermeulen et al. 2008). With the exception of iontophoresis, all these methods increase skin permeability by disrupting the stratum corneum or creating new microchannels. One of the most promising approaches is the use of microneedles (Prausnitz 2004; Prausnitz and Langer 2008; Vandermeulen et al. 2008). Microneedles provide a minimally invasive means to deliver molecules into the skin by creating microholes in the stratum corneum without inducing pain (Kaushik et al. 2001). Since the first studies in 1998 (Henry et al. 1998), new microfabrication tools have been used to manufacture microneedles made of silicon, metal or biodegradable molecules (Chabri et al. 2004; Gill and Prausnitz 2007; Park et al. 2005). Hollow microneedles allowing

the injection of small volumes of liquid have also been investigated (Wang et al. 2006; Roxhed et al. 2008). Microneedle technology, when used with biocompatible materials, is relatively safe. Moreover, insertion of both solid and hollow microneedles is not associated with pain (Kaushik et al. 2001; Sivamani et al. 2009).

Various enhancement techniques could be used in combination with microneedles in order to further improve the delivery of the drug. These techniques include iontophoresis (Lin et al. 2001; Vemulapalli et al. 2008), radio frequencies and electroporation (Hooper et al. 2007; Prausnitz and Langer 2008). In particular, the electroporation of tissues involves the application of high-voltage pulses of very short duration. This application of high-voltage electric pulses to tissue leads to cell membrane permeabilization and electrophoresis of large charged molecules. Electroporation is one of the most effective in vivo nonviral techniques to deliver DNA (Bodles-Brakhop et al. 2009; Mir 2009), although it is invasive and can induce muscle contraction (Miklavcic et al. 2005). The efficiency of the combination of high- and low-voltage pulses for DNA electrotransfer has been demonstrated (Pavselj and Préat 2005; André et al. 2008). The association of microneedle application with electroporation could result in an efficient and less painful technique for drug and DNA delivery. Namely, hollow conductive microneedles could be used for (1) painless intradermal injection without conventional needles and (2) electric pulse application leading to electric field causing electroporation in the superficial layers of the skin.

The aim of the study was thus to check if an array of hollow microneedles could be used to both inject the active substance into the skin and deliver high-voltage pulses for electroporation of the skin. First, disruption of the stratum corneum by microneedle insertion was demonstrated. The delivery of drugs, including macromolecules, was then studied in vitro and in vivo. Finally, the combination of intradermal injection and electroporation for plasmid DNA transfection in the skin was investigated.

Materials and Methods

Animals/Skin

Eight-week-old female NMRI mice from the Université Catholique de Louvain were used for the in vivo experiments. For immunization study, we used BALB/c mice that were 6 weeks old at the beginning of the experiment (Janvier, Le Genest St Isle, France). All experimental protocols on mice were approved by the Ethical Committee for Animal Care and Use of the faculty of Medicine of the Université Catholique de Louvain.

For the in vitro experiments, porcine ears were collected in a slaughterhouse. Skin from the external face of the porcine ear was removed and dermatomed to an average thickness of 500 µm (Robbins Instruments, Chatham, NJ). The use of porcine ears was authorized by the Institut Bruxellois pour la Gestion de l'Environnement (IBGE, ref. 000241692).

Microneedles and Vibratory Inserter

Hollow microneedle matrices made of Radel® R (Solvay Advanced Polymers, Alpharetta, GA) were produced by conventional micromachining followed by a deposit of gold for electrical conductivity. Beveled microneedles were 1,200 µm long and 250 µm at the base. Matrices were made of 36 microneedles, 20 solid microneedles on the edges and 16 hollow microneedles in the center (Fig. 1). The distance between the microneedles was 1 mm.

As the microneedles also serve as electrodes, the next fabrication step was to make them conductive because Radel is an insulating material. Since the conductive layer was to be applied on tridimensional objects, sputtering was chosen as a deposit method using an MP series sputter (Plassys, Marolles en Hurepoix, France). Gold was chosen as a conductive layer for its biocompatible nature and high

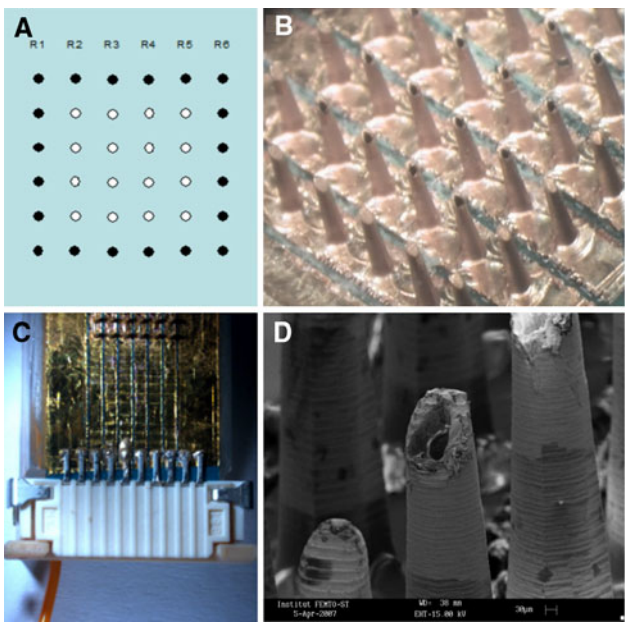

Fig. 1 **a** Schematic representation of the microneedle array. Plain microneedles (*filled circle*) and hollow microneedles (*open circle*) connected to the microreservoir. **b** Photograph showing both hollow needles in the middle and plain microneedles at the edge. **c** Photograph of the system with microneedle array and reservoir. **d** Scanning electron micrograph of the microneedle tips after tenths of penetrations

electrical conductivity ($\rho = 3.42 \times 10^{-8}\ \Omega\ m^{-1}$). A layer of titanium was used as an adhesion layer to facilitate gold deposition on the microneedles. Titanium was preferred to widely used chromium because of biocompatibility concerns. Since Radel is a highly water-adsorbent material, components had to be heated to 60°C before the deposit step. A third layer of titanium was deposited as an adhesion layer for the last insulating layer. Gold and titanium layers were then milled to form the electrical tracks. The last step of fabrication consisted of a deposit of silicon oxide to insulate electrical tracks from the skin. The needles and the end of the electrical tracks were protected by a thin film of Photoresist, which allowed them to be conductive. Afterward, Photoresist was removed by bathing the microneedles in acetone and then in ethanol. The microneedles were then rinsed in deionized water and bathed in TFTN titanium etchant (Transene, Danvers, MA) for 1 mn and then rinsed.

For pulse application, the microneedles were connected to a modified Cliniporator (IGEA, Carpi, Italy). A 10-way FFC/FPC connector, with a zero insertion force (ZIF) feature (Molex, Bievres, France), was glued onto the array, with silver conductive epoxy glue, to allow connection with the Cliniporator through a 10-way ribbon cable (Fig. 1c).

Hollow microneedles were connected to the microfluidics reservoir to allow fluid injection. The microfluidic system was developed by the SATIE Laboratory (Hoel et al. 2008). This system was made of Sylgard 184, a thermo-cross-linkable polydimethylsiloxane (PDMS). It was composed of a matrix of reservoirs covered with a deformable PDMS membrane to expel their content. It was produced by the soft lithography technique developed by Whitesides and Xia (1998). A polymethylmethacrylate (PMMA) box containing the microneedle array, the microfluidic system and the electrical connections was equipped with a semirigid polyamide capillary for the pneumatic activation of the microreservoirs. Air pressure of 20 kPa was provided with a conventional syringe. Air pressure on this membrane was responsible for fluid infusion through hollow microneedles.

To facilitate the insertion of microneedles into the skin, a vibratory inserter was used. The vibratory inserter was based on the V201/3-PA 25E shaker from Ling Dynamic Systems (Royston, UK). The shaker was powered by a Li-Po battery through an AOP541 from Burr-Brown (Tucson, AZ). The whole system was controlled by a PIC 16F877 microcontroller, which was able to synthesize, using software, any sine wave from 20 to 1.2 kHz and from 0 to ± 10 V in amplitude. Vibration duration and injection duration could be modified and controlled easily by the use of a microcontroller. Moreover, the vibratory inserter monitored the pressure applied by the microneedles on the skin. Insertion parameters were as follows: pressure 100 kPa, frequency 400 Hz, vibration time 30 s, injection time 30 s, overlap of vibration and injection 10 s.

Transepidermal Water Loss

Transepidermal water loss (TEWL) of dermatomed porcine skin was measured with a TM300 Tewameter (Courage-Khazaka, Köln, Germany) at room temperature and controlled humidity (35% RH). The microneedles were used with the vibratory inserter. TEWL was also measured in vivo on mice over 24 h after application of the microneedles with the vibratory inserter.

Passive Diffusion Enhancement

Microneedles were inserted in dermatomed porcine skin using the vibratory inserter. After that, skin samples were placed in Franz's diffusion cells with 1.5 cm^2 skin area, a 0.5 ml donor reservoir and a 1.5 ml receptor compartment at 37°C. The donor compartment was filled with a solution containing 5 mg/ml of both metoprolol and propranolol in citrate buffer (pH 3, 50 mM). The amount of both substances diffusing passively through the skin pierced by the microneedles was measured in the receiver compartment over a period of 5 h. The drugs were quantified using a high-performance liquid chromatography (HPLC) system consisting of an Agilent (Palo Alto, CA) 1100 Series Separation module and photodiode array detector, equipped with a Nucleodur RP 100-5 C18 column. The mobile phase consisted of an aqueous citrate buffer (pH 3, 50 mM) and an organic phase of methanol and acetonitrile (40:40:20, v/v). The injection volume was 50 µl, and elution was performed at a flow rate of 1.0 ml/min. The wavelength of the detector was 222 nm. The intraday and interassay variances were <5% for 12.5 µg/ml. The calibration curves were linear ($r^2 > 0.999$) over the concentration range studied (2.5–100 µg/ml). The flux (µg cm^{-2} h^{-1}) was calculated as the amount transported (µg cm^{-2}) divided by the time (h).

Bioluminescence Imaging

One microgram of luciferase was injected into the skin of NMRI mice with microneedles (10 µl) or a 30G needle for intradermal injection (1 µg/10 µl). Immediately after, 100 µl of luciferin (30 mg/ml; Xenogen, Hopkinton, MA) was injected intraperitoneally. Ten minutes later, images were acquired with a Xenogen IVIS system (IVIS 50). Photon emission was collected over a period of 60 s. Results were expressed in photons per second.

Immunization Studies

BALB/c mice were injected intradermally with 1 μg in 10 μl of ovalbumin protein with either microneedles or a 30G needle. Similarly, two boosts were applied 2 and 4 weeks after priming. Two weeks after the last boost, blood samples were collected by retro-orbital puncture and sera were separated by centrifugation. Anti-ovalbumin antibodies were measured by ELISA as previously described (Vandermeulen et al. 2009).

Reporter Gene Expression After Eletrotransfer Using Microneedles

The microneedles were inserted in the skin with the vibratory inserter, and 10 μg of pVAX-CMV-LUC in 10 μl ultrapure water were injected. An adapted Cliniporator was connected to the microneedle matrices for electrotransfer. A regular Cliniporator was used for electrotransfer with plate electrodes. Fifty micrograms in 30 μl of DNA were injected with a 30G syringe. Electrical parameters were as follows: HV 700 V/cm, 100 μs; LV 150 V/cm, 400 ms or 8 × 50 ms at 1 Hz for plate electrodes and microneedles, respectively. Pulses were delivered between the first and third rows and between the third and sixth rows of needles, respectively. The reason for this pulsing protocol was to assure a high enough (permeabilizing) electric field in the vicinity of the tips of the hollow microneedles, located between the pulse delivering rows of microneedles (see Fig. 1a for schematic representation of the microneedle array). Plasmid concentration is the highest at the tips of the hollow microneedles, and achieving permeabilizing electric field strength in those areas was crucial for a successful electrotransfer.

pVAX-CMV-LUC plasmid encoding luciferase was used as a reporter gene. Luciferase expression was detected ex vivo after tissue grinding (TD 20/20 luminometer; Promega, Madison, WI). Samples were cut into pieces and homogenized in 1 ml cell culture lysis reagent solution (CCLR, Promega Benelux) containing a protease inhibitor cocktail (Roche, Mannheim, Germany) using a Duall® tissue grinder (Cofraz, Essene, Belgium). After centrifugation at 12,000 × *g* for 10 min at 4°C, we assessed luciferase activity in 10 μl of supernatant (diluted in CCLR if needed) after addition of 50 μl of Luciferase Assay Substrate (Promega), using the TD-20/20 luminometer (Vandermeulen et al. 2007). The results were expressed in relative light units (RLUs).

Laser Doppler Imaging

A laser Doppler Imager (LDI; Moor, Devon, UK) was used to measure cutaneous blood flow on mice abdomens after insertion of the microneedle electrodes and delivery of electric pulses (HV 700 V/cm, 100 μs; LV 150 V/cm, 8 × 50 ms at 1 Hz). Measurements were performed 1, 30, 60 and 120 min and 24 h posttreatment. Pretreatment values were used as control. Data were normalized by dividing the blood flow in the region of interest (ROI) by the blood flow in the vicinal and untreated region. Results were expressed as the ratio of these values.

Modeling of the Electric Field in the Skin

Electric field and electric current calculations were made by means of commercially available Multiphysics 3.3 software (COMSOL, Los Angeles, CA) based on a finite element method. Three layers of skin were modeled: stratum corneum, viable skin and subcutaneous layer (fat and connective tissue). By taking advantage of its symmetry, only a part of the whole geometry was modeled to save computer time. Boundary conditions on the section planes were set accordingly (electric insulation on the vertical section planes). The numerical model was nonlinear, and the electric field distribution (the model output) depended on the changes in the electrical conductivity of the tissues involved (model input parameters). During the finite model analysis, tissue conductivities were changed according to the electric field distribution throughout the model. The process of tissue electropermeabilization was thus modeled in discrete time steps. In each step, the current solution was used to look for the areas where the electric field was above the predefined threshold. The conductivity of those areas was changed (increased), and the next step of the modeled electropermeabilization process was computed. This process was repeated until the electric field distribution reached its steady state (Pavselj and Miklavcic 2008).

Results and Discussion

Microneedles

In order to obtain conical microneedles of 1.2 mm height and 250 μm base diameter, we used conventional micromachining. This technique allows the drilling and milling of tender material, such as Radel, a polyphenylsulfone polymer. Radel was chosen for its biocompatibility, ease of processing and relative affordability. First, the hole (70 μm diameter) of the needles was drilled, and then microneedles were formed and beveled at 45° by milling (Fig. 1b). Because mechanical constraints during insertion are more important on the edge of the matrix, solid microneedles were placed at the border of the array for more robustness; hollow microneedles were located in the center (Fig. 1a, b).

The microneedles were electrically conductive and connected to a Cliniporator electroporation device through a FFC/FPC connector and a 10-way ribbon cable (Fig. 1c). Even though Radel is a resistant material, the repeated use of the microarrays induced the blunting and the breaking of some of the microneedles (Fig. 1d).

Disruption of the Skin Barrier by the Microneedles

To determine if the microneedles affected the skin barrier, pierced the skin and created microchannels, TEWL was measured both in vitro and in vivo (Bal et al. 2008). Passive diffusion of drugs through skin was also studied in vitro to demonstrate the increase in skin permeability.

TEWL was measured and used to assess skin barrier function in vivo on mice before, immediately after and 24 hours after application of the microneedles. As shown in Fig. 2, TEWL was enhanced after the microneedle insertion into the skin, confirming that the barrier function was impaired. Because TEWL was back to normal values after 24 h (Fig. 2b), the damage induced in vivo to the barrier was transient.

Our previous studies have shown that the vibratory inserter was required to pierce the skin (data not shown). In

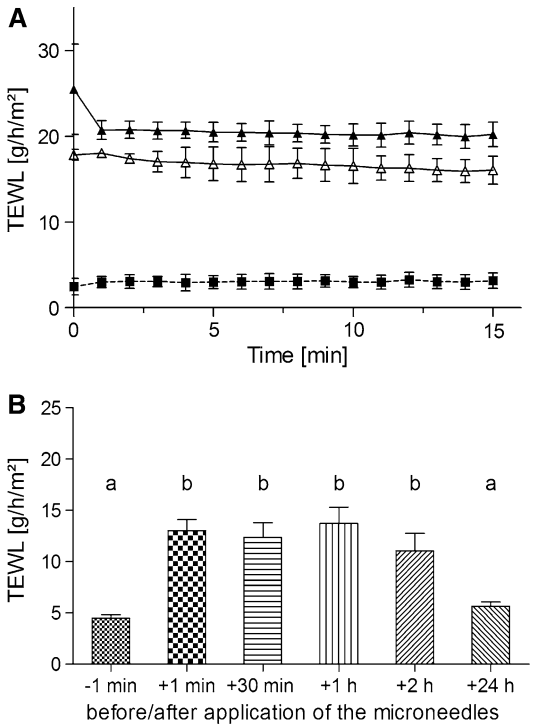

Fig. 2 **a** TEWL of porcine ear skin in vitro. (*filled square*) Negative control, (*filled triangle*) 30G needle, (*open triangle*) microneedles (mean ± SEM, $n = 6$). **b** TEWL of murine skin in vivo (mean ± SEM, $n = 6$). Groups with different superscripts differ significantly (Kruskall-Wallis $P < 0.01$)

2008, Verbaan et al. also demonstrated that the piercing of microneedle arrays in skin was improved by an impact insertion method. The duration and frequency of the vibrations did not significantly influence skin permeation. The microneedle insertion in the skin was always performed with vibration to facilitate the disruption of the stratum corneum and the penetration of microneedles. The selected parameters were as follows: frequency 400 Hz, vibration time 30 s. When a solution was injected, the injection time was 30 s, with an overlap of 10 s with vibration.

To further confirm that the microneedles were piercing the skin and increasing its permeability, microneedles were inserted in dermatomed porcine ear skin before measurement of the passive diffusion of two beta-blockers (metoprolol [log $P_{(o/w)}$ 1.9] and propranolol [log $P_{(o/w)}$ 1.2]) in the receiver compartment of Franz's diffusion cells. Pretreatment of dermatomed porcine skin with the microneedle matrix using the vibratory inserter for 15 s resulted in significantly higher passive diffusion of both drugs compared to passive diffusion through untreated skin ($P < 0.05$) (Fig. 3). Similar patterns for both drugs suggest a rapid migration of the drugs through hydrophilic microholes regardless of the physicochemical properties of the compounds. These structures have been shown by various techniques such as dye staining, histology, scanning electron microscopy, electrical resistance and TEWL measurements (Henry et al. 1998; Oh et al. 2008; Chabri et al. 2004; Martanto et al. 2004; Kolli and Banga 2008). Drug fluxes through the skin during the first hour were 25.9 ± 5.0 μg cm^{-2} h^{-1} for metoprolol and 24.8 ± 3.5 μg cm^{-2} h^{-1} for propranolol. The fluxes from the second to the sixth hour for metoprolol and propranolol were 2.1 ± 0.7 and 2.1 ± 0.5 μg cm^{-2} h^{-1}, respectively. In comparison, fluxes through untreated skin were 0.4 ± 0.1 and 0.2 ± 0.4, respectively. The decrease in the drug fluxes observed after 1 h ($P < 0.001$ for both drugs) was probably due to the resealing of these microholes. This phenomenon is related to the viscoelastic character of the skin (due to proteins such as collagen) and not to active cellular processes to repair the stratum corneum. Nevertheless, this reversible closure of the microchannels could be advantageous for the safe use of microneedle-based technology.

Macromolecule Delivery In Vivo by Microneedles

To demonstrate that the array of hollow microneedles could be used to deliver drugs into the skin in vivo, the microneedles were used to inject (1) a model protein luciferase and (2) a model antigen ovalbumin.

To check if the microneedles could be used to inject macromolecules in the skin, luciferase was used as a model

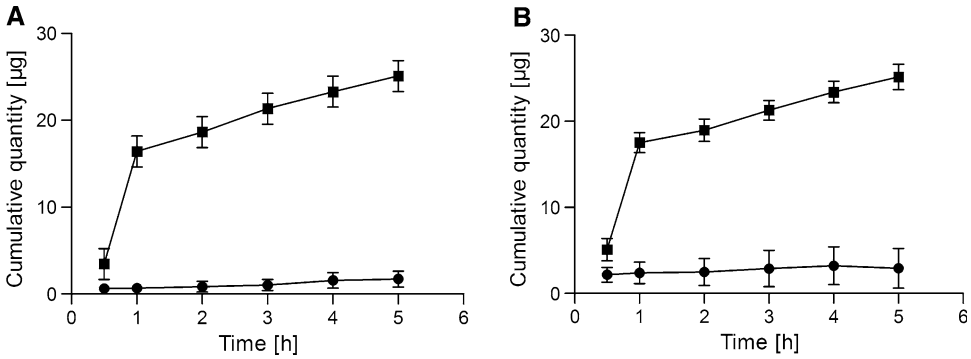

Fig. 3 Cumulative amount in micrograms (mean ± SEM, $n = 6$) of metoprolol (**a**) and propranolol (**b**) measured in the receiver compartment. Without (*filled circle*) and with (*filled square*) microneedle pretreatment

protein. As the substrate of the bioluminescence reaction, i.e., luciferin, was injected intraperitoneally and since ATP is needed for the reaction, the emission of photon is related to the presence of the model protein inside the body, revealing the achievement of the microinjection through the skin. The bioluminescence signal was equivalent when luciferase was injected with the microneedles and with conventional intradermal injection (Fig. 4a) (Mann–Whitney $P > 0.05$).

After the proof of concept, obtained with luciferase, we investigated whether an immune response could be induced after protein injection with the microneedles. Ovalbumin was used as a model antigen. The injection of ovalbumin through microneedles induced an immune response in Balb/c mice. This response, however, was lower than the one induced by intradermal injection (Fig. 4b). This could be explained by an incomplete injection of the solution contained in the microreservoir, resulting in a lower amount of protein delivered. However, this lower response could also result from a difference in the localization of the antigen in the skin.

Combination of Microneedle Insertion and Electroporation

LDI was performed to evaluate the effect of the application of microneedles and/or electroporation on the cutaneous blood flow, which is an indicator of local irritation. A transient local irritation following microneedle application with or without electric pulses was observed (Fig. 5a). These results are consistent with those obtained by Bal et al. (2008) after insertion of solid and hollow microneedles in human volunteers. In addition, application of electric pulses increased the cutaneous blood flow after 30 min to 24 h, which is consistent with previous studies (Dujardin et al. 2002).

As the microneedles can reproducibly inject macromolecules in the skin, we then studied the dual functionality of our microneedle array, i.e., injection and electroporation.

The combination of high-voltage (HV) and low-voltage (LV) pulses has been shown to be more efficient than HV or LV pulses only (Pavselj and Préat 2005; André et al.

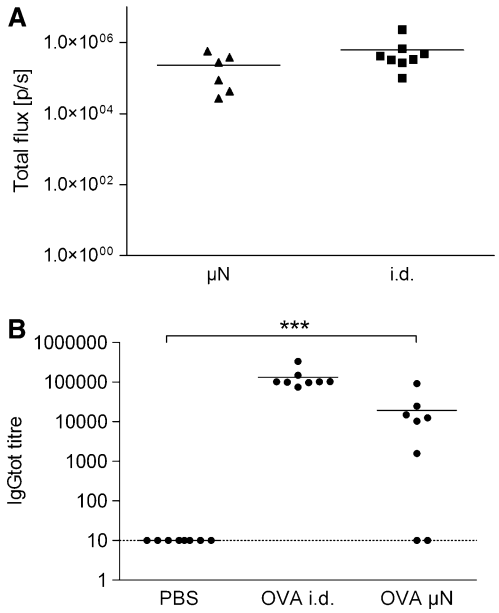

Fig. 4 **a** Bioluminescence signal after injection of luciferase with the microneedles (µN) or intradermal (i.d.) 30G needle. **b** Total IgG titers after immunization with three deliveries of 1 µg of ovalbumin, at 2-week interval. PBS vs. OVA µN, *** $P < 0.001$

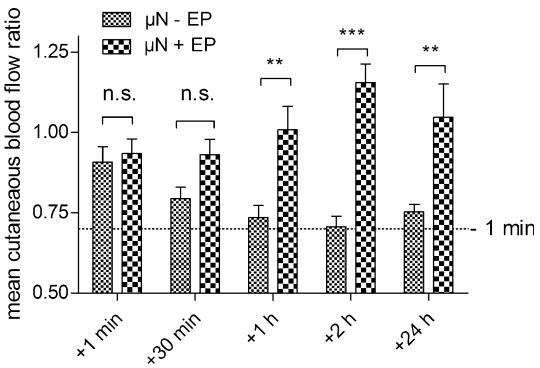

Fig. 5 Laser Doppler measurement of cutaneous blood flow after application of microneedles with or without electric pulses. *Dotted line* represents the mean blood flow 1 min before treatment. ANOVA **$P < 0.01$, ***$P < 0.001$

2008). Hence, one HV pulse (700 V/cm 100 µs) was followed by LV pulse(s) (150 V/cm 400 ms). When the microneedle array was used as electrodes, the LV pulse was fractionated to avoid burning the skin due to the poor heat conductivity of Radel microneedles. Namely, polyphenylsulfone, the material microneedles are made of, is thermally and electrically insulating. Finite element analyses of resistive heating using plate and needle electrodes was reported by Lackovic et al. (2009). The study shows that the temperature increase during a long LV pulse cannot be neglected, especially when needle electrodes are used. Therefore, the LV pulse should be fractioned into eight pulses of 50 ms at 1 Hz, to allow tissue cooling in between the pulses. On the other hand, metallic plate electrodes are good heat sinks and can ipso facto prevent skin overheating, and a single 400 ms LV pulse could be safely delivered.

Treatment parameters (means and amount of pVAX-CMV-LUC injection, pulse parameters) as well as ex vivo results of luciferase expression are summarized in Table 1. RLUs indicate the presence of luciferase in the sample.

RLUs were below quantification level when using microneedle arrays to inject DNA, regardless of the electrode type. Several different factors could be responsible for this. (1) The quantity of injected DNA was limited because of the small volume of the microreservoirs (10 µl). However, lower doses of DNA were shown to produce detectable levels of luciferase after skin electrotransfer (Vandermeulen et al. 2007). (2) Plasmid diffusion could be limited due to the small volume injected, the high viscosity of the DNA solution or the tissue compression. The plasmid could stay close to the microneedle tips, where the electric field conditions are not optimal for electrotransfer. (3) Microneedles failed to penetrate the skin. This could be due to the repeated use of microneedle arrays. Namely, they were reused several times and could progressively lose their sharpness or break as shown in Fig. 1d.

When microneedles were used to apply the electric pulses, no increase in luciferase expression was observed, although expected. This could be due to (1) the design of the pulse application, i.e., between rows 1 and 3 and rows 3 and 6 (however, several other protocols did not result in luciferase expression [data not shown]) or (2) the low electric field or the unfavorable distribution of the electric field. However, it has been reported that plain microneedles coated with dry DNA vaccine and used to apply electrical pulses could induce an immune response (Hooper et al. 2007).

To determine if the absence of transfection efficiency after injection and electroporation with the microneedles was due to a poor distribution of the electric field, in silico models developed by Pavselj et al. (2007) provided some information. The pulse parameters and the tissue-electrode geometry and conductivity dictate the distribution of the electric field during pulse delivery (Fig. 6). As already mentioned, the pulsing protocol was delivered twice: between the first and the third rows in the microneedle array (the permeabilizing HV pulse amplitude was 140 V) and between the third and the sixth rows (the permeabilizing HV pulse amplitude was 210 V). Both cases were modeled with finite elements, but only the latter is shown in Figs. 6 and 7 as the same conclusions can be drawn from both. As tissue becomes permeabilized, its conductivity is increased (Fig. 7). Before interpreting the results shown in Figs. 6 and 7, it must be stressed that the areas where good tissue permeabilization is crucial are around the tips of the hollow microneedles, where plasmid is delivered. It is evident from the model that the tissue around the pulse delivering needles becomes fully permeabilized (Fig. 7, dark red color) with the electric field in some crucial areas (microneedles in row number 3 are delivering both electric pulses and the plasmid) even exceeding the irreversible electroporation threshold. On the other hand, the electric field around the tips of the hollow microneedles between the pulse delivering ones is too low to permeabilize the tissue. Even though the needles are electrically inactive, these conductive bodies have an influence on the distribution of the electric field, causing very low values around the tips of these injecting needles.

Table 1 Luciferase expression in the skin after PVAX-CMV-LUC intradermal injection by microneedles or 30G needle and electrotransfer with plate electrodes or microneedles

Means of injection	Electrodes	DNA amount	Electrical parameters	RLU
30 G needle	Plate	50 µg	700 V/cm, 100 µs 150 V/cm, 400 ms	884 ± 442
30 G needle	Microneedles	50 µg	700 V/cm, 100 µs 150 V/cm, 8 × 50 ms, 1 Hz	53.5 ± 13.3
Microneedles	Microneedles	10 µg	700 V/cm, 100 µs 150 V/cm, 8 × 50 ms, 1 Hz	n.d.
Microneedles	Plate	10 µg	700 V/cm, 100 µs 150 V/cm, 400 ms	n.d.
30 G needle	None	50 µg	n.a.	100 ± 65[a]

n.d. not detectable, *n.a.* not applicable

[a] Vandermeulen et al. (2007)

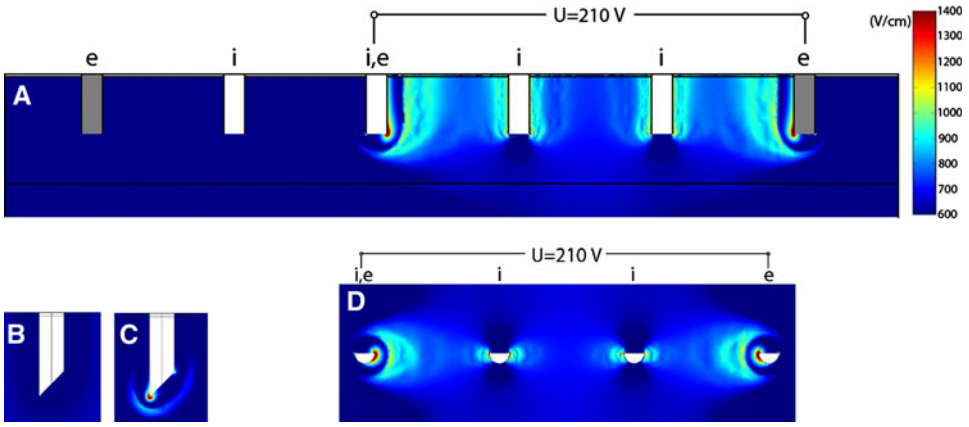

Fig. 6 In silico model of field distribution microneedle array electrodes in the skin. Electroactive (*e*) needles and injecting (*i*) needles. The pulses (amplitude is 210 V) are in this case delivered between the two rows of electrodes as shown. The electric field distribution is shown in **a** 2D *x–y* plane, cut through the microneedles; **b** 2D *z–y* plane, cut through nonpulse delivering microneedles; **c** 2D *z–y* plane, cut through a pulse delivering microneedle; **d** 2D *z–x* plane, cut through the beveled microneedle tips. The tissue is permeabilized when exposed to electric fields approximately in the range 600–1400 V/cm (Color figure online)

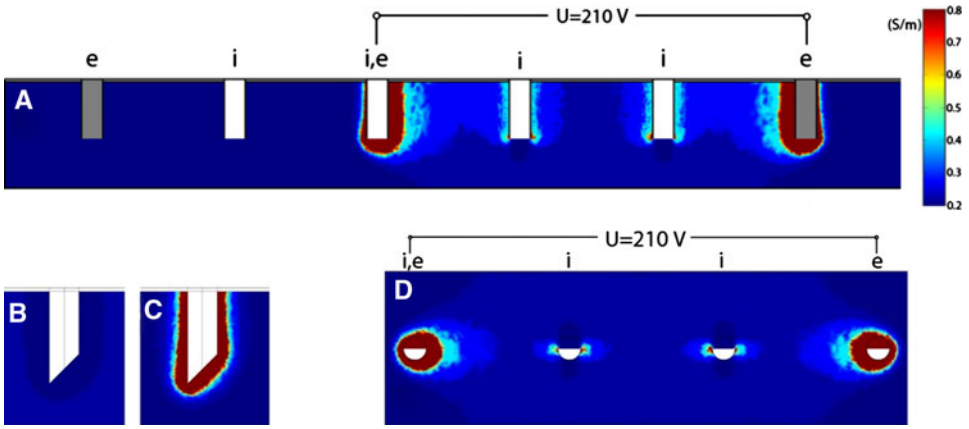

Fig. 7 In silico model of tissue conductivity of microneedle array electrodes in the skin. Electroactive (*e*) needles and injecting (*i*) needles. The pulses (amplitude is 210 V) are in this case delivered between the two rows of electrodes as shown. The conductivity of the tissue is shown in **a** 2D *x–y* plane, cut through the microneedles; **b** 2D *z–y* plane, cut through a nonpulse delivering microneedle; **c** 2D *z–y* plane, cut through a pulse delivering microneedle; **d** 2D *z–x* plane, cut through the beveled microneedle tips. The areas marked in red are fully permeabilized, while the areas marked in dark blue are completely nonpermeabilized (Color figure online)

Conclusion

We evaluated whether hollow conductive microneedles could be used both for drug injection and for skin electroporation. Gold-coated Radel microneedle arrays were assessed for stratum corneum disruption and injection of various model drugs as well as their use as electrodes for electric pulse application. We demonstrated proper insertion features of these microneedles in combination with a vibratory inserter. We obtained a proof of concept that these arrays allow for effective injection of proteins into the skin, resulting in an immune response directed to the model antigen, ovalbumin. However, electrotransfer of plasmid DNA using the microneedles to inject the DNA or as electrodes to apply the pulses showed several limitations of the setup. The first is the limited amount of DNA that can be delivered because of the small volume of the microreservoirs or high DNA viscosity. Therefore, it is important that the microfluidic reservoir of the microneedle array is enlarged. A second concern regarding electrotransfer with our microneedles is the electric field distribution. Needle electrodes produce less favorable electric field distribution than plate electrodes. This can result in an irreversible electroporation of the cells near the tips of the microneedles delivering the pulses and less than adequate electroporation farther away from the electrodes. In addition, the electric field distribution is perturbed by the nonactivated needles, resulting in an electric field insufficient for electrotransfer. To ensure an optimal electric field at the site where DNA is injected by the microneedles, the

electric field should be applied between each row of microneedles at lower electrical fields to achieve cell permeabilization without reaching the irreversible electroporation threshold. Further investigation is needed to understand this phenomenon and optimize the injection and electrical parameters for efficient electrotransfer.

Acknowledgments Are addressed to the UE sixth framework program and the Angioskin consortium (LSH-2003-512127) that made this work possible.

References

André FM, Gehl J, Sersa G et al (2008) Efficiency of high- and low-voltage pulse combinations for gene electrotransfer in muscle, liver, tumor, and skin. Hum Gene Ther 19:1261–1271

Bal SM, Caussin J, Pavel S et al (2008) In vivo assessment of safety of microneedle arrays in human skin. Eur J Pharm Sci 35:193–202

Bodles-Brakhop AM, Heller R, Draghia-Akli R (2009) Electroporation for the delivery of DNA-based vaccines and immunotherapeutics: current clinical developments. Mol Ther 17:585–592

Chabri F, Bouris K, Jones T et al (2004) Microfabricated silicon microneedles for nonviral cutaneous gene delivery. Br J Dermatol 150:869–877

Dujardin N, Staes E, Kalia Y et al (2002) In vivo assessment of skin electroporation using square wave pulses. J Control Release 79:219–227

Gill HS, Prausnitz MR (2007) Coated microneedles for transdermal delivery. J Control Release 117:227–237

Henry S, McAllister DV, Allen MG et al (1998) Microfabricated microneedles: a novel approach to transdermal drug delivery. J Pharm Sci 87:922–925

Hoel A, Baron N, Cabodevila G et al (2008) Microfluidic distribution system for an array of hollow microneedles. J Micromech Microeng 18:065019

Hooper JW, Golden JW, Ferro AM, King AD (2007) Smallpox DNA vaccine delivered by novel skin electroporation device protects mice against intranasal poxvirus challenge. Vaccine 25: 1814–1823

Kaushik S, Hord AH, Denson DD et al (2001) Lack of pain associated with microfabricated microneedles. Anesth Analg 92:502–504

Kolli CS, Banga AK (2008) Characterization of solid maltose microneedles and their use for transdermal delivery. Pharm Res 25:104–113

Lackovic I, Magjarevic R, Miklavcic D (2009) Three-dimensional finite-element analysis of joule heating in electrochemotherapy and in vivo gene electrotransfer. IEEE Trans Dielec Elec Insul 16:1338–1347

Lin W, Cormier M, Samiee A et al (2001) Transdermal delivery of antisense oligonucleotides with microprojection patch (Macroflux) technology. Pharm Res 18:1789–1793

Martanto W, Davis SP, Holiday NR et al (2004) Transdermal delivery of insulin using microneedles in vivo. Pharm Res 21:947–952

Miklavcic D, Pucihar G, Pavlovec M et al (2005) The effect of high frequency electric pulses on muscle contractions and antitumor efficiency in vivo for a potential use in clinical electrochemotherapy. Bioelectrochemistry 65:121–128

Mir LM (2009) Nucleic acids electrotransfer-based gene therapy (electrogenetherapy): past, current, and future. Mol Biotechnol 43:167–176

Oh JH, Park HH, Do KY et al (2008) Influence of the delivery systems using a microneedle array on the permeation of a hydrophilic molecule, calcein. Eur J Pharm Biopharm 69: 1040–1045

Park JH, Allen MG, Prausnitz MR (2005) Biodegradable polymer microneedles: fabrication, mechanics and transdermal drug delivery. J Control Release 104:51–66

Pavselj N, Miklavcic D (2008) Numerical modeling in electroporation-based biomedical applications. Radiol Oncol 42:159–168

Pavselj N, Préat V (2005) DNA electrotransfer into the skin using a combination of one high- and one low-voltage pulse. J Control Release 106:407–415

Pavselj N, Préat V, Miklavcic D (2007) A numerical model of skin electropermeabilization based on in vivo experiments. Ann Biomed Eng 35:2138–2144

Prausnitz MR (2004) Microneedles for transdermal drug delivery. Adv Drug Delivery Rev 56:581–587

Prausnitz MR, Langer R (2008) Transdermal drug delivery. Nat Biotechnol 26:1261–1268

Roxhed N, Griss P, Stemme G (2008) Membrane-sealed hollow microneedles and related administration schemes for transdermal drug delivery. Biomed Microdevices 10:271–279

Sivamani RK, Stoeber B, Liepmann D et al (2009) Microneedle penetration and injection past the stratum corneum in humans. J Dermatol Treat 20:156–159

Vandermeulen G, Staes E, Vanderhaeghen ML et al (2007) Optimisation of intradermal DNA electrotransfer for immunization. J Control Release 124:81–87

Vandermeulen G, Daugimont L, Préat V (2008) DNA transfer in the skin. In: Walters KA, Roberts MS (eds) Dermatologic, cosmeceutic and cosmetic development: therapeutic and novel approaches. Informa Healthcare, New York, pp 537–555

Vandermeulen G, Daugimont L, Richiardi H et al (2009) Effect of tape stripping and adjuvants on immune response after intradermal DNA electroporation. Pharm Res 26:1745–1751

Vemulapalli V, Yang Y, Friden PM et al (2008) Synergistic effect of iontophoresis and soluble microneedles for transdermal delivery of methotrexate. J Pharm Pharmacol 60:27–33

Verbaan FJ, Bal SM, van den Berg DJ et al (2008) Improved piercing of microneedle arrays in dermatomed human skin by an impact insertion method. J Control Release 128:80–88

Wang PM, Cornwell M, Hill J et al (2006) Precise microinjection into skin using hollow microneedles. J Invest Dermatol 126: 1080–1087

Whitesides GM, Xia Y (1998) Soft lithography. Annu Rev Mater Sci 28:153–184